Neuron
Article

Regional Slow Waves and Spindles in Human Sleep

Yuval Nir,[1] Richard J. Staba,[2] Thomas Andrillon,[1,4] Vladyslav V. Vyazovskiy,[1] Chiara Cirelli,[1] Itzhak Fried,[3,5] and Giulio Tononi[1,*]
[1]Department of Psychiatry, University of Wisconsin-Madison, Madison, WI 53719, USA
[2]Department of Neurology
[3]Department of Neurosurgery and Semel Institute for Behavioral Neuroscience
David Geffen School of Medicine, University of California, Los Angeles, Los Angeles, CA 90095, USA
[4]Department of Cognitive Studies, Ecole Normale Superieure, 75005 Paris, France
[5]Functional Neurosurgery Unit, Tel Aviv Medical Center and Sackler School of Medicine, Tel Aviv University, Tel Aviv 64239, Israel
*Correspondence: gtononi@wisc.edu
DOI 10.1016/j.neuron.2011.02.043

SUMMARY

The most prominent EEG events in sleep are slow waves, reflecting a slow (<1 Hz) oscillation between up and down states in cortical neurons. It is unknown whether slow oscillations are synchronous across the majority or the minority of brain regions—are they a global or local phenomenon? To examine this, we recorded simultaneously scalp EEG, intracerebral EEG, and unit firing in multiple brain regions of neurosurgical patients. We find that most sleep slow waves and the underlying active and inactive neuronal states occur locally. Thus, especially in late sleep, some regions can be active while others are silent. We also find that slow waves can propagate, usually from medial prefrontal cortex to the medial temporal lobe and hippocampus. Sleep spindles, the other hallmark of NREM sleep EEG, are likewise predominantly local. Thus, intracerebral communication during sleep is constrained because slow and spindle oscillations often occur out-of-phase in different brain regions.

INTRODUCTION

Sleep is defined by behavioral unresponsiveness and is usually regarded as a global phenomenon. Indeed, sleep is accompanied by global changes in neuromodulation (Jones, 2005), and the transition from waking to sleep is accompanied by clear-cut changes in the electroencephalograph (EEG): from low-amplitude high-frequency activity to high-amplitude low-frequency slow waves (<4 Hz) and sleep spindles (Steriade, 2000).

Intracellular recordings indicate that sleep slow waves reflect a bistability of cortical neurons undergoing a slow oscillation (<1 Hz) between two distinct states, each lasting hundreds of milliseconds. Up states are associated with depolarization and vigorous firing, whereas in down states, the membrane potential is hyperpolarized and neuronal firing fades (Contreras and Steriade, 1995; Crunelli and Hughes, 2010; Destexhe and Contreras, 2006; Destexhe et al., 2007; Steriade et al., 1993c, 2001; Timofeev et al., 2001). Although a role has been suggested for thalamic oscillators (Crunelli and Hughes, 2010), the slow oscillation can be generated and sustained in cerebral cortex alone (Amzica and Steriade, 1995a; Shu et al., 2003; Steriade et al., 1993a; Timofeev et al., 2000; Timofeev and Steriade, 1996). The slow oscillation affects virtually all neocortical neurons (Amzica and Steriade, 1995b; Chauvette et al., 2010; Sejnowski and Destexhe, 2000); it is remarkably synchronous when examined in brain slices (Sanchez-Vives and McCormick, 2000), in animals under anesthesia (Steriade et al., 1993b,1993c), and in natural sleep, as shown by intracellular recordings of up to four neurons simultaneously (Chauvette et al., 2010; Volgushev et al., 2006). But are slow oscillations truly global events (i.e., occurring in phase across most brain regions), or can the slow oscillation occur locally (i.e., in a minority of regions independently of other brain areas)?

Recent observations have shown that slow waves can be locally regulated so that their intensity varies among cortical regions. Prolonged waking induces an increase in slow wave activity (SWA; EEG power <4 Hz), which is largest over frontal cortex (Finelli et al., 2001; Werth et al., 1997). High-density EEG (hd-EEG) demonstrates that sleep slow waves can be locally regulated as a function of prior use and plastic processes (Esser et al., 2006; Huber et al., 2004, 2006). Slow waves propagate along major anatomical pathways (Massimini et al., 2004; Murphy et al., 2009) so that individual waves may be driven by distinct cortical origins (Riedner et al., 2007). Additional evidence for local sleep goes beyond local regulation of slow waves in non-rapid eye movement (NREM) sleep. For example, when falling asleep, cortical activity is highly variable across brain regions (Magnin et al., 2010). Moreover, in natural sleep of some animals (e.g., dolphins), one hemisphere can be awake while the other is asleep (Mukhametov et al., 1977). Finally, in humans, some sleep disorders (e.g., sleep walking) suggest the existence of "dissociated states" (Mahowald and Schenck, 2005), where some brain regions are "asleep" when others are simultaneously "awake."

Given the recent evidence supporting local regulation of SWA, we hypothesized that sleep slow waves may occur locally such that neurons alternate between active and inactive states at different times in different brain regions. To evaluate this possibility, simultaneous recordings of intracranial depth EEG and spiking activities of isolated units were obtained in 8–12 brain

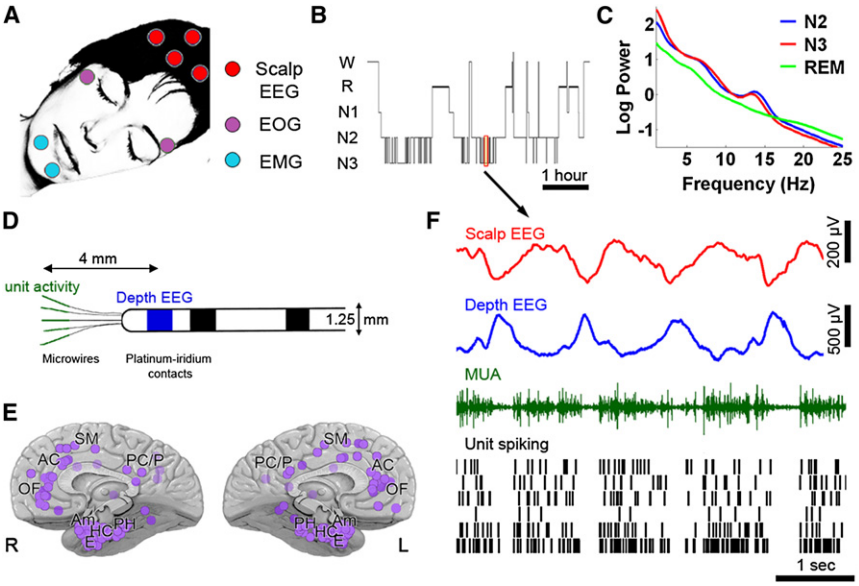

Figure 1. Sleep Studies and Data Overview

(A) Set-up for polysomnographic sleep recordings.

(B) Hypnogram: time-course of sleep-wake stages in one representative individual. W, wake; R, REM sleep; N1-N3, NREM sleep, stages 1–3.

(C) Average power spectra of scalp EEG in the same individual computed separately in stages N2 (blue), N3 (red) and REM sleep (green). Note high power in slow wave (<4 Hz) and spindle (10–16 Hz) range in NREM sleep.

(D) Diagram of flexible probes used for concomitant recording of depth EEG (platinum contacts, blue) and unit activity (microwires, green).

(E) Overview of 129 depth electrode locations in 13 individuals encompassing multiple brain regions seen from medial view. Abbreviations: OF, orbitofrontal cortex; AC, anterior cingulate; SM, supplementary motor; PC/P, posterior cingulate / parietal cortex; PH, parahippocampal gyrus; HC, hippocampus; E, entorhinal cortex; Am, amygdala; L, left hemisphere; R, right hemisphere.

(F) Example of data acquired during 6 s of NREM sleep. Rows (top to bottom) show activity in scalp EEG (Cz, red), depth EEG (entorhinal cortex, blue), multiunit activity (MUA) in one microwire (green), and spiking activity in six isolated single-units (black bars).

regions in the cortex and hippocampus of 13 individuals undergoing presurgical clinical testing. The results provide direct evidence for local slow waves, revealing a continuum of global-local waves, with the majority of events being confined to specific regions. At one extreme, typical of early NREM sleep, high-amplitude slow waves were usually global, detectable with scalp EEG. At the other extreme, more typical of late NREM sleep, slow waves could be entirely local, where any region could be active or inactive. In addition, we find that sleep spindles—the other EEG hallmark of NREM sleep—also occur mostly locally, establishing that the two fundamental sleep oscillations are mostly confined to local circuits. We also reveal a robust tendency of sleep slow waves to propagate from medial prefrontal cortex to the medial temporal lobe (MTL) and hippocampus. Both local occurrence and propagation of slow wave events reflect the underlying connectivity such that transitions into activity in a given region can be predicted by the activity of its afferent regions.

RESULTS

Polysomnographic Sleep Studies and Sleep Slow Waves

We obtained full night continuous polysomnographic sleep recordings in 13 neurosurgical patients, lasting 421 ± 20 min (mean ± SEM). Figure 1 illustrates the experimental setup and provides an overview of the data. Polysomnography included electrooculogram (EOG), electromyogram (EMG), scalp EEG, and video monitoring. Sleep-wake stages were scored as waking, NREM sleep stages N1 through N3, and REM sleep according to established guidelines (Iber et al., 2007). Depth intracranial electrodes recorded activity in 129 medial brain regions in frontal and parietal cortices, parahippocampal gyrus, entorhinal cortex, hippocampus, and amygdala (Figure 1E; see Table S1A available online). We simultaneously recorded scalp EEG, depth EEG, multiunit activity (MUA), and neuronal spiking activity (Figure 1D) from a total of 600 units (355 single units and 245 multiunit clusters).

Measures of overnight sleep in patients resembled normal sleep in individuals without epilepsy (Figure S1). Average (±SEM) sleep efficiency (sleep time per time in bed) was 82% ± 2%. NREM sleep, REM sleep, and wake after sleep onset (WASO) constituted 75% ± 2%, 13% ± 2%, and 12% ± 2% of sleep time, respectively. Moreover, power spectra of scalp EEG data in individual subjects (Figure 1C; Figure S1) revealed robust SWA and spindle (10–16 Hz) power throughout NREM sleep, while REM sleep was characterized by power in the theta (4–8 Hz) range and in high frequencies (>20 Hz), in accordance with previous studies (Campbell, 2009). All patients showed typical NREM-REM sleep cycles, and some showed homeostatic decline of SWA throughout sleep. These results indicate that sleep measures were in general agreement with typical findings in healthy young adults (e.g., Riedner et al., 2007).

Having characterized sleep using standard noninvasive polysomnography, individual slow waves in NREM sleep were identified in the depth EEG of each brain region separately. Although sleep profiles were within the normal range, we further verified that detected waves reflected physiological sleep slow waves rather than epileptic events (Experimental Procedures). Putative slow waves were separated to those preceded (within 1 s) by an interictal spike (“paroxysmal” discharges) versus those unrelated to epilepsy (“physiological” sleep slow waves). The shape of physiological sleep slow waves was symmetrical and significantly different than that of asymmetrical paroxysmal discharges (Figure S2A). Specifically, in paroxysmal slow waves following interictal spikes, the rise slope was 44% ± 0.07% steeper than the fall slope (n = 129 depth electrodes; $p < 7.4 \times 10^{-5}$, paired

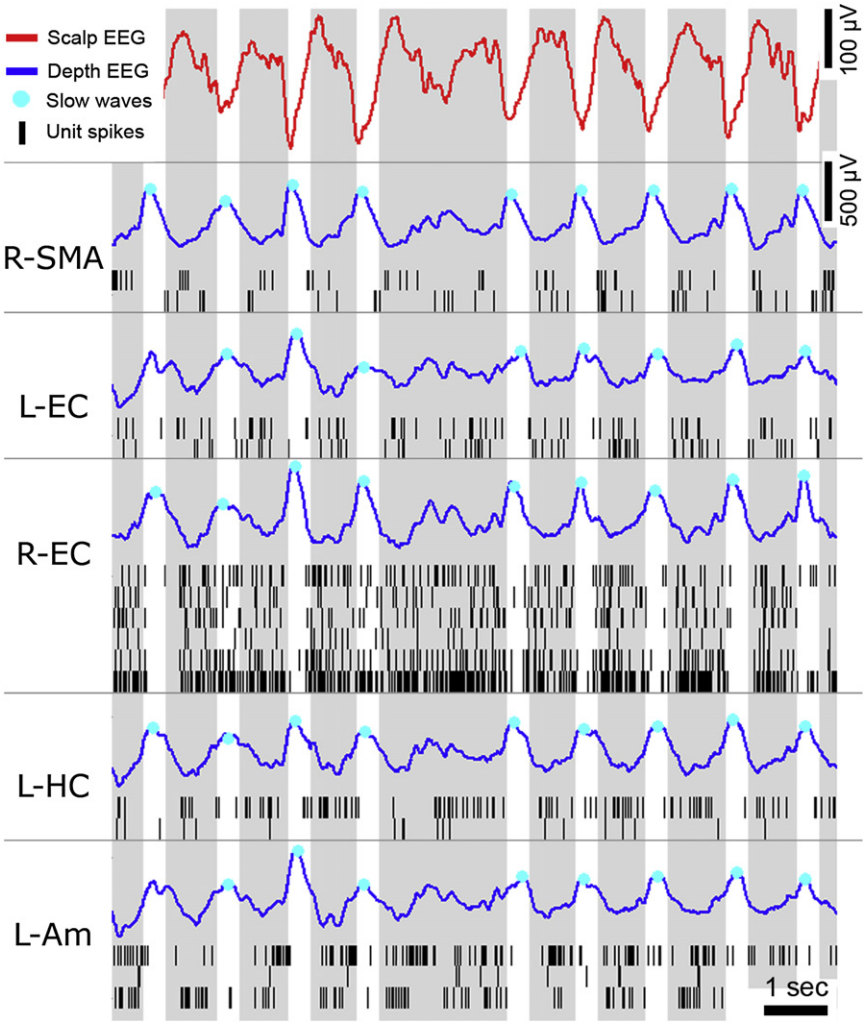

Figure 2. Example of EEG and Single-Unit Activity During Global Sleep Slow Waves

Example of EEG and unit activities in multiple brain regions during 11.5 s of deep NREM sleep in one individual. Rows (top to bottom) depict activity in scalp EEG (Cz), right supplementary motor area (R-SMA), left entorhinal cortex (L-EC), right entorhinal cortex (R-EC), left hippocampus (L-HC), and left amygdala (L-Am). Red, scalp EEG; blue, depth EEG; black lines, unit spikes. Cyan dots show individual slow waves detected automatically in each channel separately. Gray and white vertical bars mark ON and OFF periods occurring in unison across multiple brain regions.

t test on rise and fall slopes). In addition, paroxysmal discharges were limited to specific sites in comparison to physiological slow waves, which were detected in all brain structures in all patients. Thus, in many channels, virtually no interictal spikes were observed before slow waves (and nearly all putative slow waves were physiological), while in a few channels many events were pathological (mean, 14%; range, 0.06%–46%). By contrast, the number of physiological slow waves was consistent between electrodes, with numbers matching those found in healthy individuals (37.3 ± 0.5 slow waves per minute of NREM sleep), as in (Riedner et al., 2007).

Neuronal Activity Underlying Sleep Slow Waves

Next, isolated unit discharges underlying physiological sleep slow waves were examined. Figure 2 provides an example of EEG and unit activities during global slow waves occurring in unison across multiple brain regions during deep NREM sleep in one individual. Negative peaks in the scalp EEG tightly corresponded to positive peaks of depth EEG in cortical and subcortical structures across different lobes and hemispheres. Locally, extracellular recordings revealed an OFF period where unit spiking activity ceased almost entirely, likely corresponding to the down state of the slow oscillations as recorded intracellularly. As in previous work (Vyazovskiy et al., 2009b), we use the terms "ON" and "OFF" periods, instead of "up" and "down" or "depolarized" and "hyperpolarized" states (Steriade et al., 2001), because activity and silence periods were defined here on the basis of extracellular activity rather than membrane potential fluctuations measured intracellularly. In contrast, positive peaks in scalp EEG tightly corresponded to negative peaks of depth EEG and to ON periods with rigorous spiking, in accordance with a depolarized up state.

We set out to examine quantitatively the relationship between sleep slow waves and the underlying spiking activity across all brain regions where units were detected (Figure 3). Individual slow waves were detected automatically in the depth EEG of each brain region separately (e.g., cyan dots in Figure 2), and unit spiking activity surrounding slow waves was averaged. When focusing on the highest amplitude waves in each channel (top 20%), positive and negative peaks in depth EEG were associated with marked decreases and increases in unit discharges, respectively (Figures 3A and 3B; n = 600). This result should be viewed as a lower limit on the modulation strength, since timing variability across individual neurons introduced a temporal jitter, thereby smearing the average result. Therefore, the wave-triggered average of spiking activity was computed in each unit separately, searching for the minimal (maximal) rate while allowing for different time offsets around EEG peaks (n = 600, average of 10,595 waves per neuron). The minimal firing rate around EEG positivity was 39% ± 1% compared with the mean firing rate in NREM (N2+N3) sleep, and the mean latency of such OFF periods was 72 ± 9 ms before the positive EEG peak. Around EEG negativity, a maximal firing rate of 198% ± 11% was found across individual units, at 46 ± 10 ms before the negative EEG peak.

In each subject and in each brain region, individual neurons whose activity was highly modulated by slow waves were

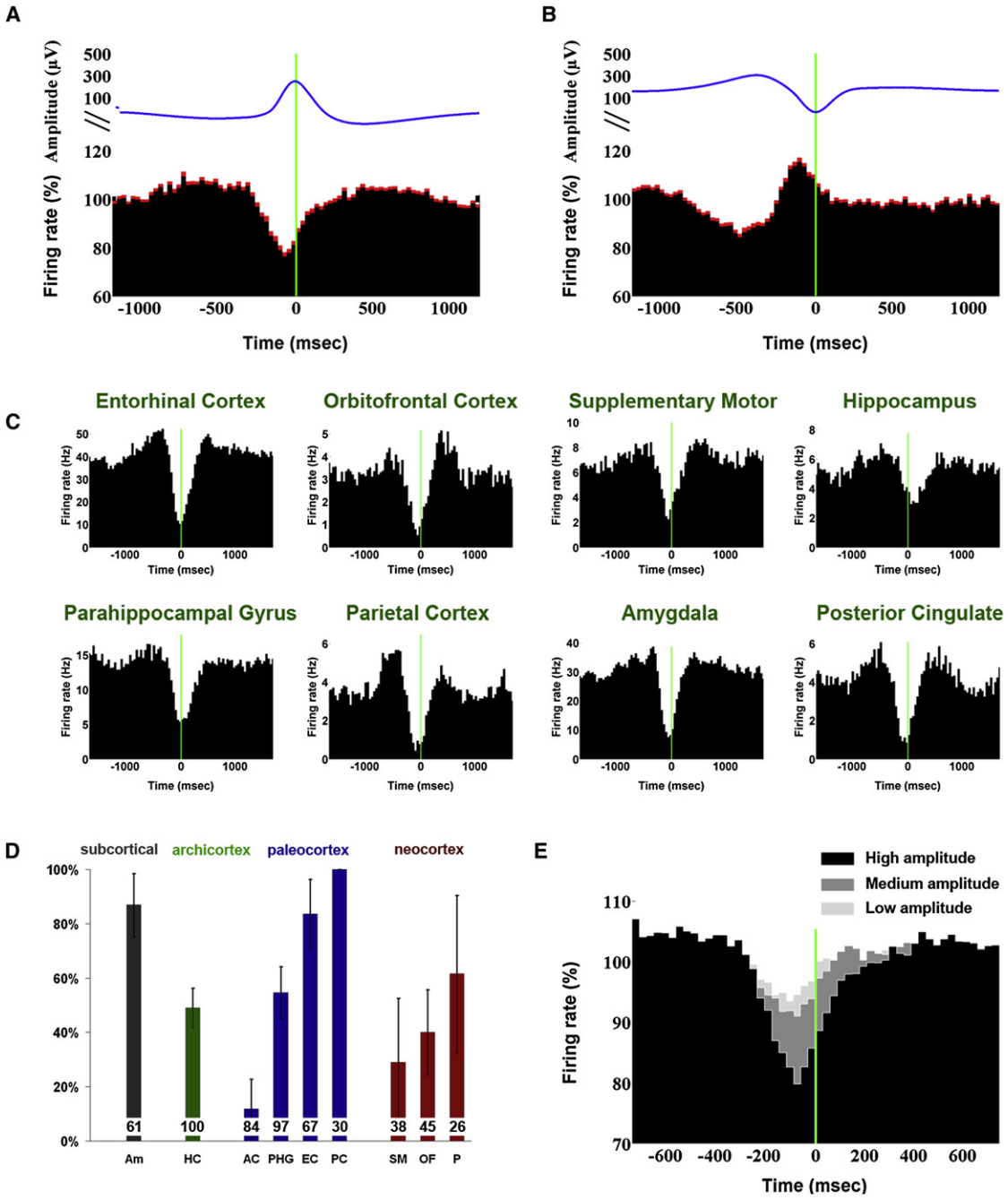

Figure 3. Spiking Activity Underlying EEG Slow Waves

(A) Wave-triggered averaging of unit spiking activity, time locked to the positive peak of depth EEG slow waves (OFF periods). Red shades denote SEM across neurons (n = 600 in all brain structures).

(B) Same as (A) time locked to the negative peak of depth EEG slow waves (ON periods).

(C) Examples of neurons in different individuals and brain structures with spiking activity highly linked to EEG slow waves.

(D) Percentage of units linked to sleep slow waves in different brain structures. Numbers at base of bars mark the number of units in each brain structure, and error bars denote SEM across electrodes.

(E) Wave-triggered averaging of units in all brain structures (n = 600) as a function of amplitude of the positive EEG peaks. Slow waves were divided into three amplitude percentiles so that black, dark gray, and light gray depict high, medium, and low-amplitude slow waves, respectively.

identified (Figure 3C). Such neurons were found not only in neocortex, but also in limbic structures such as hippocampus and amygdala. Given the variability across individual neurons, we examined the percentage of neurons showing significant phase locking to sleep slow waves separately in each brain structure (Figure S3; see Experimental Procedures). The results revealed considerable variability (Figure 3D): the lowest percentages of phase locked neurons were found in anterior cingulate (12% ± 11%, n = 84 units in 11 regions, mean and SEM across electrodes). Neocortical regions (41% ± 11%, n = 109 units in 16 regions), hippocampus (49% ± 7%, n = 100 units in 17 regions), and parahippocampal gyrus (55% ± 10%, n = 97 units in 13 regions) showed intermediate effects, while the highest percentages of phase locked neurons were found in the amygdala (87% ± 11%, n = 61 units in 9 amygdala regions), entorhinal cortex (84% ± 13%, n = 67 units in 10 regions), and posterior cingulate cortex (100% ± 0%, n = 30 units in three regions). Since slow waves were detected in the depth EEG recorded ~4 mm away from unit activity, the percentages of modulated neurons should be regarded as a lower bound. Given that slow wave amplitudes change throughout sleep with the dissipation of sleep pressure (Riedner et al., 2007), it was of interest to check whether slow wave amplitudes were indicative of the level of unit activity modulation. To this end, unit activities were averaged around slow waves depending on the peak amplitude of the depth EEG (Figure 3E). The amplitude of EEG waves was parametrically related to the degree of modulation in underlying unit activity. Thus, our results demonstrate that within specific brain structures, sleep slow waves in depth EEG reliably reflect synchronous transitions between ON and OFF periods among many neurons.

Importantly, unit discharges associated with pathological waves were markedly different in that firing rate was significantly different before and after the EEG positivity, in accord with the asymmetry observed in depth EEG (Figure S2B). The clear distinction found in spiking activity underlying physiological versus pathological waves supports the notion that sleep slow waves and epileptic events could be reliably separated.

Extent of Local Sleep Slow Waves

Next we examined whether, to what extent, and under what circumstances slow waves occur locally (i.e., out of phase between brain regions). We operationally define a local (global) slow wave as an event detected in less (more) than 50% of recording locations. Numerous incidences of regional slow waves were found (Figure 4A; see Figure S4 for additional examples). In such incidences, diverse measurements (depth EEG, MUA, and spiking of individual neurons) jointly indicated that one brain region was in an OFF period while another region was active.

To explore this phenomenon quantitatively we examined to what extent slow waves occurred nearly simultaneously (±400 ms) across multiple brain structures and in scalp EEG. For each wave, the underlying unit activity at concordant sites (i.e., where the same EEG wave was observed) was compared with that found in nonconcordant sites (i.e., where the "seed" wave was not observed in the "target" region). The results (Figure 4B) revealed a clear difference in underlying spiking activity ($p < 6.8 \times 10^{-7}$, paired t test between concordant and nonconcordant conditions across neurons).

We quantified the number of brain structures involved in each slow wave (i.e., the number of channels in which a particular wave was detected). The distribution of involvement was skewed toward fewer regions (Figure 4C) indicating that slow waves were typically spatially confined. Mean slow wave involvement was 27.1% ± 0.4% of monitored brain regions (n = 129 electrodes). Moreover, 85% ± 0.7% of slow waves were detected in less than half of the recording sites indicating that most slow waves were local, given the definition above. There was a strong tendency ($r = 0.79$; $p << 1 \times 10^{-10}$) of widespread waves to be of higher amplitude than spatially restricted lower-amplitude waves (Figure 4D). The high variability in amplitude and spatial extent of slow waves suggests a continuum rather than a categorical dichotomy between local and global waves. At one extreme, waves could be entirely local, where one region was ON and others were OFF and vice versa, and such local waves could be observed in any brain structure. At the other extreme, high-amplitude waves occurred in unison across the brain. Nearly all waves fell somewhere along this gradual continuum, with most waves being more local than global given our working definition. Finally, we examined whether specific pairs of brain structures had a strong tendency to express local slow waves concordantly and whether particular brain regions had a strong degree of involvement in slow waves (Figure 4E). Medial prefrontal regions, such as the anterior cingulate and orbitofrontal cortex, were typically more involved than regions in MTL. In addition, homotopic cortical regions across hemispheres tended to be concordant in prefrontal cortex (but not MTL), and there was a slight bias of regions in the left hemisphere to be more involved in slow waves.

Extent of Local Sleep Spindles

Our results thus far demonstrate that slow waves, the most prominent EEG event of NREM sleep, occur mostly locally. This finding suggests that sleep, which usually is associated with highly synchronized activity, has an important local component. We thus wondered whether sleep spindles, the other hallmark of NREM sleep EEG (Loomis et al., 1935), also occur locally. Spindles are generated in the highly interconnected thalamic reticular nucleus, and the neocortex governs their synchronization through corticothalamic projections (McCormick and Bal, 1997; Steriade, 2003). Asynchronous spindles were reported in nonphysiological conditions (Contreras et al., 1996, 1997; Gottselig et al., 2002).

To examine this issue, spindles were detected automatically in each depth electrode separately (Experimental Procedures; Figure S5), and we examined to what extent spindles occurred concurrently across frontal and parietal channels. Examination of local versus coincident spindles was performed only in cortical sites that had regular spindle occurrences, thereby excluding the possibility that local occurrence of spindles arises merely from their total absence in remote brain structures. As defined for slow waves, we operationally define a local (global) sleep spindle as an event detected in less (more) than 50% of recording locations. Numerous incidences of sleep spindles occurring in specific brain areas were found (Figure 5A). Regional spindles occurred without spindle activity in other regions, including homotopic regions across hemispheres and regions with equivalent signal-to-noise ratio (SNR) showing the same slow waves.

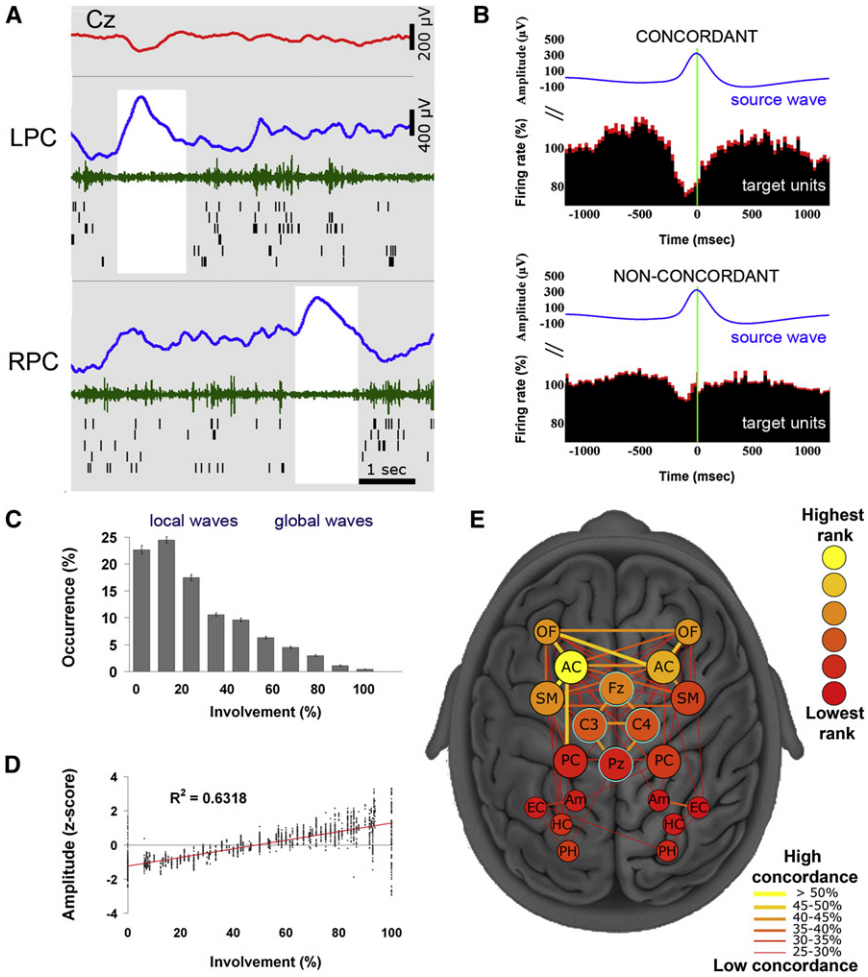

Figure 4. Local Sleep Slow Waves

(A) An example of local sleep slow waves occurring at different times in left and right posterior cingulate cortices, where 100% of units are locked to slow waves. Rows (top to bottom) depict activity in scalp EEG (Cz, red), left posterior cingulate, and right posterior cingulate. Blue, depth EEG; green, MUA; black lines, single-unit spikes. White shadings mark local OFF periods.

(B) Units in concordant "target" regions (expressing the same EEG slow wave, upper panel) exhibit a clear OFF period, while units in nonconcordant "target" regions do not exhibit a clear OFF period. Wave-triggered averaging of "target" units is time locked to the positive peak of depth EEG in the "seed" region (blue trace). Red shades denote SEM across neurons (n = 410 in all brain structures).

(C) Most slow waves are local. Distribution of slow wave involvement (percentage of monitored brain structures expressing each wave) is shown.

(D) Global slow waves are of high amplitude. Scatter plot shows slow wave amplitudes as a function of involvement (percentage of brain structures expressing each wave).

(E) A graph depicting the tendency of each pair of regions to express waves concordantly. Nodes (individual regions) are depicted schematically as seen from above, where deep regions away from scalp (MTL) are smaller and scalp electrodes are surrounded by cyan. Node color (legend) denotes the rank of each region—that is, how often it is involved in slow waves seen in other regions. Edge width and color (legend) denotes the probability of each pair of regions to express slow waves concordantly. Note that regions in prefrontal cortex have higher ranks and show concordance across hemispheres relative to MTL.

We set out to quantitatively establish to what extent local sleep spindles occur across the entire dataset. We determined for each spindle in a given region whether spindles were present or not in other brain structures (Experimental Procedures). The spectral power changes in concordant sites (34% of events where a spindle was detected in both "seed" and "target" channels; Figure 5B top row) were compared with those at nonconcordant sites (66% of events where a spindle was detected in the seed channel but not in the target, Figure 5B bottom row). A clear difference in spectral power was revealed ($p < 1 \times 10^{-41}$, paired t test), pointing to significant differences in underlying neuronal activity, and indicating that nonconcordant events are indeed regional spindles. Furthermore, the analysis of those cases where target channels did not exhibit any increase in spindle spectral power above the noise level (Experimental Procedures) revealed that 32% of all nonconcordant events were local in the strongest sense—that is, a full-fledged spindle occurred in the seed channel while spectral power in the target channel was not different from chance. Importantly, the occurrence of local spindles was independent of local slow waves, since spindles occurring in isolation (i.e., not associated with a slow wave within ± 1.5 s) constituted 53.7% ± 3.1% of all events and 79.8% ± 0.8% of such "isolated" spindles were detected in less than 50% of brain regions. In addition, comparing homotopic regions revealed that 40.4% ± 1.7% of spindles were observed only in one hemisphere (mean ± SEM across nine pairs), indicating that differences between anterior and posterior regions could not account for spindle locality.

Next, we quantified the involvement in spindle events by computing the number of brain structures in which each spindle was observed. The distribution of involvement in sleep spindles was skewed toward fewer regions (Figure 5C), indicating that spindles were typically spatially restricted. Mean involvement for sleep spindles was 45.5% ± 0.3% of brain regions (n = 50 depth electrodes). Moreover, 75.8% ± 0.9% of spindles were detected in less than 50% of regions, indicating that most spindles were local given the definition above. Finally, as was the case for slow waves, the spatial extent of spindles was significantly correlated with spindle amplitude (Figure 5D; r = 0.62; $p < 0.0001$; n = 177).

Changes in Spatial Extent of Slow Waves and Spindles between Early and Late Sleep

Increasing evidence suggests that early and late NREM sleep differ substantially in underlying cortical activity (Vyazovskiy

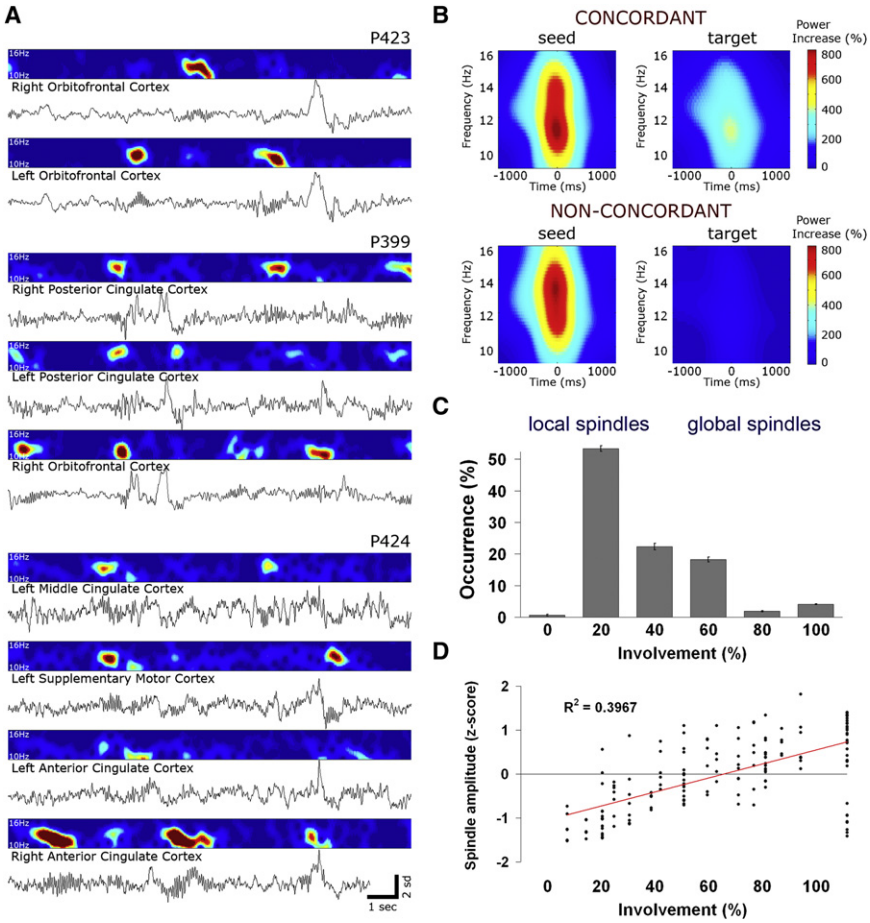

Figure 5. Local Sleep Spindles

(A) Three examples in three different patients of depth EEG along with corresponding spectrograms in the spindle frequency range (10–16 Hz) during 15 s of NREM sleep. Note that, regardless of slow waves, local spindles often occur without spindle activity in other regions, including homotopic regions across hemispheres and regions with equivalent SNR showing the same global slow waves.

(B) Quantitative analysis of spindle occurrence across pairs of channels. Top row (concordant events, 34% of cases) shows spectrograms for events in which a spindle was detected in the "seed" channel but not in the "target" channel (N = 13,750 events in 156 pairs of regions in 12 individuals). Bottom row (nonconcordant events, 66% of cases) shows spectrograms for events in which a spindle was detected in the seed channel but not detected in the target channel (N = 26,874 events in 156 pairs of regions in 12 individuals). Note that spindle power in nonconcordant target channels is at near-chance levels, indicating that our detection can reliably separate between presence and absence of spindle activity.

(C) Distribution of involvement (percentage of monitored brain structures expressing each spindle) is shown across 22,914 spindles in 50 electrodes of 12 individuals. Note that the distribution is skewed to the left, indicating that most spindles are local.

(D) Scatter plot of spindle amplitudes as a function of involvement (percentage of brain structures expressing each spindle) shows that global spindles have some tendency to be of higher amplitude ($r = 0.63$; $p < 0.0001$; $n = 177$).

et al., 2009b). Hence, it was of interest to determine whether the spatial extent of slow waves and spindles changes between early and late NREM sleep. To this end, we focused on episodes of early and late NREM sleep in five individuals exhibiting a clear homeostatic decline of SWA during sleep (Figure S1). We identified separately slow waves, spindles, and K-complexes, which are isolated high-amplitude slow waves that are triggered by external or internal stimuli on a background of lighter sleep (Colrain, 2005). We examined for each type of sleep event separately how its spatial extent varied between early and late sleep (Figure 6). Slow waves became significantly more local in late sleep as compared to early sleep (Figure 6A, involvement of 30.4% ± 0.57% in early sleep versus 25.0% ± 0.62% in late sleep; $p < 2.6 \times 10^{-10}$, unequal variance t test). This result is in line with the finding that local waves were usually low amplitude, and low-amplitude waves typically occur in late NREM sleep when homeostatic sleep pressure has largely dissipated (Riedner et al., 2007). By contrast, K-complexes were mostly global and stereotypical throughout the night—that is, they did not show significant changes between early and late sleep (Figure 6B; involvement of 54.8% ± 4.4% in early sleep versus 52.5% ± 1.9% in late sleep; $p = 0.98$). Interestingly, sleep spindles became slightly less local in late sleep, as sleep pressure dissipated (Figure 6C; involvement of 44.2% ± 0.6% in early sleep versus 47.1% ± 0.5% in late sleep; $p < 0.00014$). This result once again supports the notion that local sleep spindles cannot be simply explained by an association with local slow waves.

Sleep Slow Waves Propagate along Typical Pathways

To examine whether slow waves propagate along typical pathways, we checked for consistent temporal delays between brain regions in which the same wave was observed. Figure 7A provides an example of mean slow waves in depth EEG of different brain structures in one individual, revealing a propagation trend from medial frontal cortex to the MTL and hippocampus. This propagation was evident also when examining the distribution of lags for individual waves (Figure 7A, right). Despite variability in the timings of individual waves, some regions consistently preceded scalp EEG whereas others followed it.

A systematic analysis of depth EEG established that slow waves had a strong propensity to propagate from medial frontal cortex to the MTL and hippocampus. Specifically, we identified all slow waves that were detected within ±400 ms across several brain structures (Experimental Procedures). Sorting regions according to the order in which their slow waves were detected revealed a clear tendency of slow waves to propagate from medial frontal cortex to the MTL (Figure 7B), which was highly significant

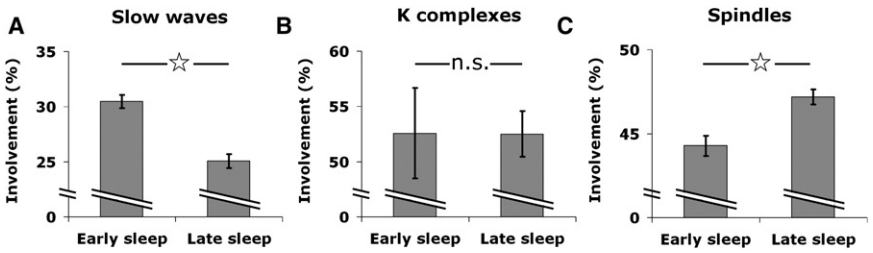

Figure 6. Changes in Spatial Extent of Slow Waves and Spindles Between Early and Late Sleep

(A) Slow waves become more local in late sleep. Slow wave involvement (percentage of monitored brain structures expressing each wave) in early NREM sleep versus late NREM sleep in five individuals exhibiting a clear homeostatic decline of SWA during sleep (Figure S1). Error bars denote SEM (n = 1436 and 1698 events in early and late sleep). Asterisk denotes statistically significant difference ($p < 2.6 \times 10^{-10}$, unequal variance t test).

(B) K complexes are more global and similar in early and late sleep. Same sleep segments and analysis as (A). Error bars denote SEM (n = 148 and 181 events in early and late sleep; p = 0.98, unequal variance t test).

(C) Spindles become more global in late sleep. Same sleep segments and analysis as (A). Error bars denote SEM (n = 1272 and 2554 events in early and late sleep, p < 0.00014, unequal variance t test).

statistically (Figure 7C; $p < 2.3 \times 10^{-8}$, unequal variance t test). In addition, this propagation tendency was consistent across individual subjects and robust to different examinations (Figure S6).

Figure 7D shows an example of individual slow waves propagating across multiple brain structures. As can be seen, time offsets in OFF periods in different brain regions followed a propagation from frontal cortex to the MTL (diagonal green lines). Next, slow wave propagation was quantitatively examined in unit discharges in all 11 individuals in whom unit recordings were obtained simultaneously in frontal and MTL regions. Mean spiking activities underlying slow waves in medial frontal cortex versus MTL revealed a robust time offset (Figure 7E, left). Across individual neurons, minimal firing in frontal neurons (n = 76) was −85 ± 22 ms relative to scalp Fz negative peak, whereas minimal firing in MTL neurons (n = 155) was +102 ± 20 ms relative to the same time reference, indicating an average difference of 187 ms (Figure 7E, right). The statistical significance of this time offset was confirmed via bootstrapping by computing time delays of individual neurons while randomly shuffling their anatomical labels ($p << 1 \times 10^{-10}$; Figure S6G). In fact, across 10,000 iterations, not even one instance was found in which a random time offset between the two groups of neurons was as high as (the real) 187 ms. Next, we examined whether within the MTL, spiking activities could also reveal a preferred direction of signal propagation between cortex and hippocampus. In 11 individuals in whom unit recordings were obtained simultaneously from multiple MTL regions, slow wave-triggered averaging of spiking activity (Figure 7F, left) revealed that slow waves occurred first in the parahippocampal gyrus, next in entorhinal cortex, and lastly in the hippocampus, emulating the anatomical pathways (see also Discussion). Across individual neurons minimal firing in parahippocampal neurons occurred −19 ± 20 ms relative to positive peak of depth EEG slow waves in MTL, while minimal firing in hippocampal neurons occurred +103 ± 47 ms relative to the same time reference, indicating that slow waves exhibited an average time difference of 122 ms between cortex and hippocampus (Figure 7F, right). The statistical significance of this time offset was confirmed via bootstrapping while randomly shuffling anatomical labels (p < 0.0097; Figure S6H).

Finally, we examined whether hippocampal sharp-wave/ripple (SWR) bursts may precede and drive responses in medial prefrontal cortex (mPFC), a primary projection zone of hippocampal output in primates (Cavada et al., 2000). To this end, we focused on seven subjects in whom hippocampal ripples were recorded simultaneously along with spiking activities in hippocampus and mPFC. Hippocampal ripples were detected, and their relationship to sleep slow waves was examined (Experimental Procedures and Figure S7). In line with previous observations (Clemens et al., 2007; Molle et al., 2006; Sirota et al., 2003), hippocampal ripples were found to occur preferentially around ON periods (Figure S7D). A fine time scale examination of spiking activities revealed that hippocampal neurons transiently elevated their firing rates around ripple occurrence (Figure S7E). Across individual hippocampal neurons (n = 72), time offsets of peak firing were −31 ± 7 ms from detected ripples (Figure S7G). Adjacent entorhinal neurons also elevated their firing rates transiently albeit to a lesser degree (Figure S7E), and time offsets were −2 ± 9 ms, indicating that they followed hippocampal neurons by 29 ms on average. By contrast, individual mPFC neurons did not show a consistent transient firing rate increase (Figure S7G). Rather, mPFC neurons only exhibited a sustained increase in firing that was significantly higher than the mean rates in NREM sleep (Figure S7E; p < 0.05, unequal variance t test), most probably because ripples occurred preferentially during ON periods. These results suggest that ripples reflect hippocampal output that is largely confined spatially to the MTL. By contrast, slow wave-triggered averaging of spiking activity in mPFC and hippocampus once again revealed that slow waves in prefrontal cortex preceded those found in hippocampus (Figure S7F). On the whole, our results suggest that signal propagation in slow wave sleep primarily follows a cortical-hippocampal direction.

Afferent Synaptic Input Predicts Occurrence and Timing of Activity Onsets in Individual Slow Waves

What determines whether and when a given region transitions into an active state? We hypothesized that this process is not entirely stochastic and is determined by what proportion of its afferents have just transitioned to an active state. To test this possibility, we focused on the amygdala and its afferents. This choice was guided by the fact that projections to the amygdala in primates are mostly ipsilateral and arrive from diverse sources, with a notable contribution from other limbic structures such as entorhinal cortex, cingulate cortex, and hippocampus, as well as medial prefrontal and orbitofrontal cortices serving mainly as input sources (Amaral et al., 1992; McDonald, 1998). We

capitalized on this anatomical organization and examined whether we could predict the occurrence and timing of individual slow waves in the amygdala. Crucially, if transitions into ON periods indeed reflect cumulative drive of anatomical afferents, we expected that we could better predict the occurrence of events on the basis of ipsilateral limbic afferents than on the basis of equivalent contralateral information.

To examine this possibility, we inspected data in 17 hemispheres of nine individuals in which signals from amygdala and several other limbic structures were recorded. A linear classifier was trained with a subset of slow waves to utilize information about the occurrence, amplitude, and timing of transitions into population ON periods (positive peaks in depth EEG) in ipsilateral (or contralateral) limbic regions to predict the occurrence and timing of individual slow waves in the amygdala (Experimental Procedures). Its performance was then tested with a separate subset of waves (Figure 8). In all nine individuals, the information from ipsilateral afferent regions led to significantly greater accuracy in predicting the occurrence of slow waves in the amygdala ($p < 1 \times 10^{-39}$ for all nine individuals). Moreover, ipsilateral prediction accuracy monotonically increased as a function of the number of afferent regions that were made available for classifier training (Figure 8A, red; slope = 0.04% ± 0.005% correct per neighbor). By contrast, contralateral prediction was sometimes at near-chance levels and did not depend as strongly on the number of regions (Figure 8A, blue; significantly smaller slopes; $p < 5.4 \times 10^{-4}$ via paired t test). Along the same line, the timing of individual slow waves in the amygdala (whether they occurred before or after the parietal scalp electrode) could be more accurately predicted with information from ipsilateral afferent regions ($p < 1.4 \times 10^{-7}$ in eight individuals and $p = 0.02$ in ninth individual, Figure 8B). Thus, despite the probabilistic nature of activity onsets in slow waves, the underlying process is not entirely stochastic and reflects the cumulative drive of afferent synaptic input.

DISCUSSION

By examining simultaneous depth EEG and single-unit recordings in multiple regions of the human brain, we show that ON and OFF periods of spiking activity and corresponding EEG slow waves typically involve a limited number of brain regions. Similarly, sleep spindles are mostly local. In addition, slow waves have a tendency to propagate from prefrontal cortex to the MTL and hippocampus. We also found that activity onsets in individual waves reflect the afferent synaptic drive to a given region.

Local Sleep Slow Waves

The main observation reported here is that most sleep slow waves are in fact confined to local regions (i.e., detected in a minority of brain areas). Specifically, in most cases we found that when some brain regions were in an ON state, neurons in other brain regions were completely silent. The unique dataset used here was instrumental in unequivocally establishing this phenomenon, since (1) the large size of the human brain facilitated simultaneous recordings across multiple distant sites, and (2) the simultaneous recording of depth EEG, MUA, and spiking of individual neurons allowed us to establish that differences between depth EEGs in different regions reflect local activities rather than noise.

Typically, less than 30% of monitored brain regions were involved in each slow wave event. Although our sampling was mostly limited to medial brain areas, it represented activity in multiple (8–12) regions across lobes and hemispheres, so it is reasonable to infer that these results can be generalized to the entire brain. When global ON and OFF states were observed, they were associated with large slow waves in scalp recordings, usually during deep sleep early in the night, or with K-complexes throughout the night. Local slow waves tended to co-occur across homotopic prefrontal regions, but not across homotopic regions in the MTL (Figure 4E), supporting the role of callosal pathways in slow wave synchronization and propagation (Amzica and Steriade, 1995a). Medial prefrontal regions including the anterior cingulate and orbitofrontal cortex were among the most involved in slow wave occurrence.

The demonstration that slow waves are mostly local shows that examples of isolated slow waves (Mohajerani et al., 2010; Sirota and Buzsaki, 2005) constitute the rule rather than the exception. It is also consistent with evidence that the intensity of sleep slow waves can vary across brain regions (Finelli et al., 2001), that sleep can be regulated locally (Huber et al., 2004, 2006), and that multiple local generators could contribute to EEG SWA (Murphy et al., 2009; Riedner et al., 2007).

Local Sleep Spindles

In physiological conditions, spindles are believed to reflect global signal propagation between cortex and thalamus (Achermann and Borbely, 1998; Contreras et al., 1996; Steriade, 2003). Although spindles are generated in the thalamus, the neocortex governs spindle synchronization through corticothalamic projections (Steriade, 2003). Asynchronous spindles were observed during development (Khazipov et al., 2004) or in nonphysiological conditions such as decortication, cortical depression, and acute stroke, where a nonfunctional cortex is not able to exert its normal synchronizing influence (Contreras et al., 1996, 1997; Gottselig et al., 2002).

By simultaneously examining spindle occurrence across multiple brain regions (Figure 5), the present results demonstrate that, like most slow waves, most sleep spindles occur locally in natural sleep. Thus, each spindle event was usually detected in only a minority of brain regions. Even when applying the most conservative criteria, treating any spindle spectral power above the noise level as a spindle event, approximately one-third of events occurred independently across regions. As found for slow waves, the spatial extent of spindles was correlated with their amplitude. Although spindles are often associated with slow wave up-states (Molle et al., 2002; Steriade et al., 1993b), spindles occurred locally in a way that was independent of local slow waves. Also, the local occurrence of spindles cuts across the distinction between fast (13–15 Hz) centroparietal spindles and slow (11–13 Hz) frontal spindles (Anderer et al., 2001), since spindles of the same frequency can occur in isolation between homotopic regions across hemispheres. It is an open question whether local and global spindles may be mediated by different mechanisms such as corticothalamic projections from different layers (Jones, 2009) or thalamocortical projections via the core

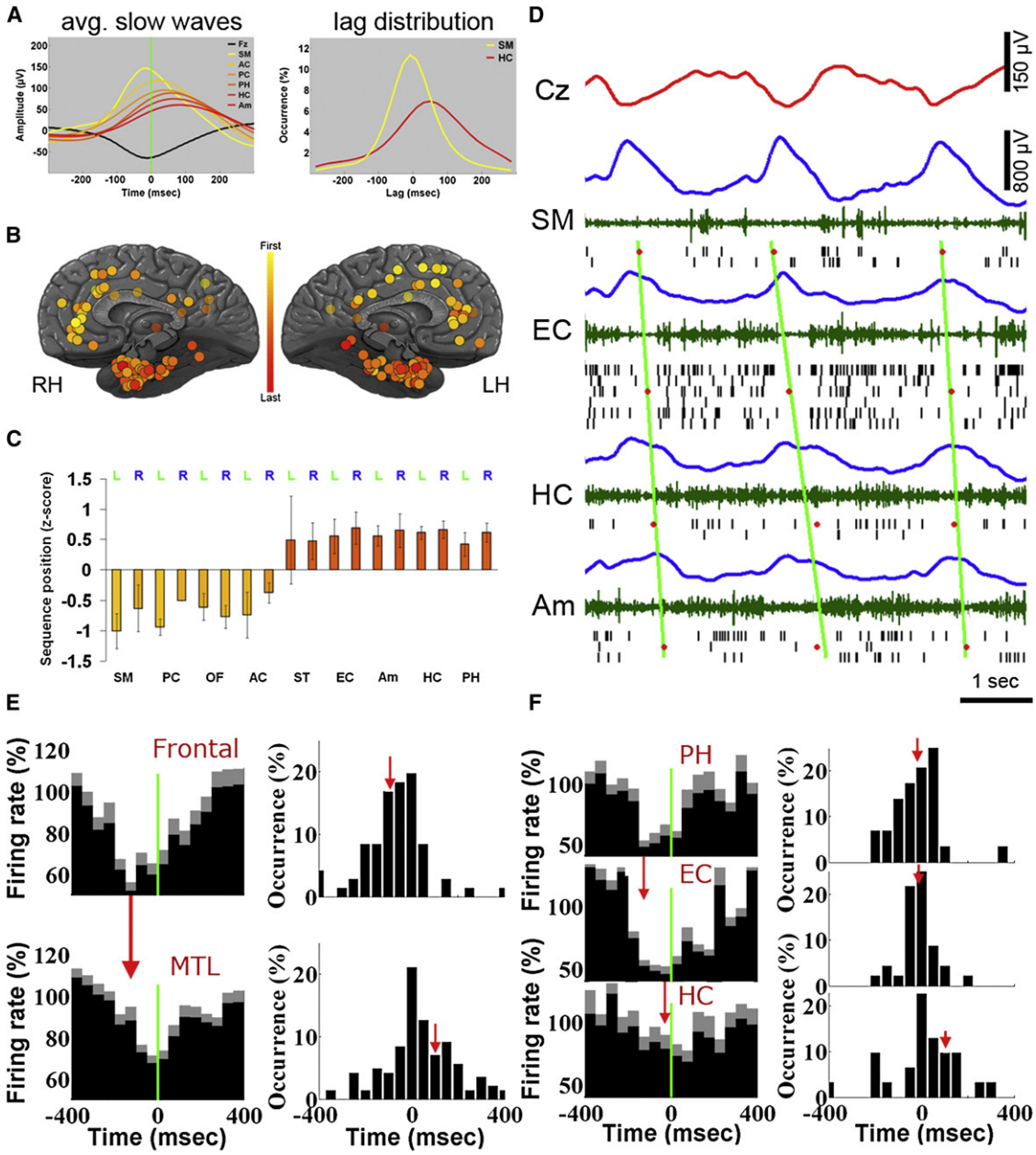

Figure 7. Sleep Slow Waves Propagate Across Typical Paths

(A) Left: Average depth EEG slow waves in different brain structures of one individual illustrate propagation from frontal cortex (yellow) to MTL (red). All slow waves are triggered by scalp EEG negativity. Black, scalp mean waveform. Right: Distributions of time lags for individual waves in supplementary motor area (SM, yellow) and hippocampus (HC, red) relative to scalp.

(B) Mean position in sequences of propagating waves in all 129 electrodes across 13 individuals. Each circle denotes one depth electrode according to its precise anatomical location. Yellow-red colors denote waves observed sooner in frontal cortex compared with MTL (see legend).

(C) Quantitative analysis: mean position in propagation sequences as a function of brain region. Abbreviations: SM, supplementary motor area; PC, posterior cingulate; OF, orbitofrontal cortex; AC, anterior cingulate; ST, superior temporal gyrus; EC, entorhinal cortex; Am, amygdala; HC, hippocampus; PH, parahippocampal gyrus.

(D) An example of individual slow waves propagating from frontal cortex to MTL. Rows (top to bottom) depict activity in scalp EEG (Cz, red), supplementary motor area (SM), entorhinal cortex (EC), hippocampus (HC), and amygdala (Am). Colors denote the following: blue, depth EEG; green, MUA; and black lines, spikes of isolated units. Red dots mark center of OFF periods in each brain region based on the middle of silent intervals as defined by last and first spikes across the local population. Diagonal green lines are fitted to OFF period times via linear regression and illustrate propagation trend.

(E) Left: The average unit activity in frontal cortex (top, n = 76) and MTL (bottom, n = 155), triggered by the same scalp slow waves reveals a robust time delay (illustrated by vertical red arrow). Right: Distribution of time delays in individual frontal (top) and MTL (bottom) units reveals a time delay of 187 ms. Red vertical arrows denote mean time offset relative to scalp EEG.

and matrix cells (Rubio-Garrido et al., 2009; Zikopoulos and Barbas, 2007).

Some previous data hinted at the possibility that sleep spindles may occur or be regulated locally. One study reported that during drowsiness spindles occurred in medial prefrontal cortex, while posterior regions showed alpha activity (Caderas et al., 1982). Another study reported that spindle power can vary and correlate with motor learning (Nishida and Walker, 2007). A recent study using noninvasive magnetoencephalography found that the average coherence between pairs of sensors was significantly lower than that found between scalp EEG (Dehghani et al., 2010), implying asynchronous generators. Indeed, the present findings demonstrate that local sleep spindles constitute the majority of events in natural human sleep.

Taken together, the finding that both slow waves and spindles are mainly confined to local regions adds to the evidence suggesting that sleep arises from activities of local circuits and is not exclusively a global phenomenon (Krueger et al., 2008). In isolated cortical slices, long periods of silence are interrupted by short bursts of activity, much like the EEG of preterm newborns (tracé alternant) (Kristiansen and Courtois, 1949). Prior use and induction of plastic changes lead to regional enhancements of SWA in human sleep (Esser et al., 2006; Huber et al., 2004, 2006) and rodent sleep (Vyazovskiy et al., 2000). In addition, local circuits may exhibit OFF periods even during wakefulness while the animal is performing a task (Vyazovskiy et al., 2011). Imaging studies demonstrate some local modulation of thalamocortical activity in slow wave sleep (Braun et al., 1997; Dang-Vu et al., 2005, 2008; Maquet, 2000). Apart from local slow waves, clinical evidence suggests the existence of "dissociated states" (Mahowald and Schenck, 2005). For example, in sleepwalking and REM sleep behavior disorder, some brain circuits may be asleep while others are awake (Bassetti et al., 2000; Mahowald and Schenck, 2005; Terzaghi et al., 2009). Naturally occurring sleep patterns in dolphins (Mukhametov et al., 1977), seals (Siegel, 2009), and birds (Rattenborg et al., 2001) also suggest that parts of the brain can be awake while others are asleep. Overall, such evidence implies that, although sleep is often considered as a global phenomenon, it may be best understood in relation to activities of local circuits.

Unit Discharges Underlying Sleep Slow Waves

A tight relationship between EEG sleep slow waves and underlying unit activity was evident in all monitored brain structures (Figures 2 and 3). Although there was considerable variability among individual neurons, in each brain region, the activity of a substantial portion of neurons was phase locked with slow waves (Figure 3D). Moreover, the amplitude of EEG slow waves reflected the degree of modulation in neuronal firing (Figure 3E). A tight relationship between EEG slow waves and underlying unit activity is a widely established phenomenon in natural sleep of mammals, as demonstrated by extracellular recordings (Amzica and Steriade, 1998; Ji and Wilson, 2007; Noda and Adey, 1970; Sirota et al., 2003; Vyazovskiy et al., 2009b), owing to the fact that within each region, the activity of different neurons is highly synchronized (Destexhe et al., 1999). In neocortex, sleep slow waves reflect a slow oscillation of membrane potential fluctuations, as demonstrated by intracellular recordings (Chauvette et al., 2010; Isomura et al., 2006; Steriade et al., 2001). Recent studies in human cortex have similarly demonstrated that slow waves reflect alternations between neuronal firing and suppressed activity (Cash et al., 2009; Csercsa et al., 2010; Le Van Quyen et al., 2010). Our results extend these observations to multiple regions in the human brain (Figure 3C). Neurons phase-locked to slow waves were found not only in neocortex, but also in limbic paleocortex (e.g., cingulate cortex, parahippocampal gyrus, and entorhinal cortex), archicortex (hippocampus), and subcortical structures (amygdala). Although neurons in subcortical structures seem to lack the inherent bistability of cortical neurons (Isomura et al., 2006), their activity is nevertheless modulated by slow oscillations generated locally or imposed by the cortex (Pare et al., 2002; Wolansky et al., 2006). Indeed, our recordings demonstrate that neurons in entorhinal cortex, hippocampus, and amygdala modulate their spiking activities in concert with EEG slow waves.

Propagation of Sleep Slow Waves and Cortico-Hippocampal Dialogue

Previous studies suggested that slow waves may have a tendency to propagate along an anterior-posterior axis through the cingulate gyrus and neighboring structures (Murphy et al., 2009), which constitute an anatomical backbone of anatomical fibers (Hagmann et al., 2008). By simultaneously recording from 8–12 brain structures directly, the current results establish that slow waves indeed propagate in the human brain as previously suggested (Massimini et al., 2004; Murphy et al., 2009), and as observed in part in rodents (Vyazovskiy et al., 2009a) and cats (Volgushev et al., 2006). The consistent tendency of slow waves to propagate along distinct anatomical pathways (e.g., cingulum) indicates that such waves can be used to investigate changes in neuronal excitability and connectivity.

By recording EEG and spiking activities from multiple adjacent MTL structures, we demonstrate that cortical slow waves precede hippocampal waves in the human brain. As far as can be inferred from medial brain structures, the results reveal a sequential cortico-hippocampal propagation of slow waves along well-known anatomical paths, from the parahippocampal gyrus, through entorhinal cortex, to hippocampus (Figure 7F), as was observed in intracellular recordings in rodents (Isomura et al., 2006). A similar cortico-hippocampal succession was revealed when focusing exclusively on hippocampus and mPFC recorded simultaneously in seven patients (Figure S7F). Our results are in line with previous animal studies (Hahn et al., 2007; Isomura et al., 2006; Ji and Wilson, 2007; Molle et al., 2006; Sirota et al., 2003) and with a recent study of human depth EEG (Wagner et al., 2010). That cortical slow waves precede hippocampal waves is also compatible with a cortical origin for sleep slow waves (Chauvette et al., 2010; Steriade et al., 1993c).

(F) Left: The average unit activity in parahippocampal gyrus (PH, n = 32), entorhinal cortex (EC, n = 49) and hippocampus (HC, n = 35), triggered by the same depth EEG slow waves reveals a cortico-hippocampal gradient of slow wave occurrence (illustrated by vertical red arrows). Right: Distribution of time delays in individual PH, EC, and HC units reveals a time delay of 121 ms between PH and HC. Red vertical arrows denote mean time offset relative to depth EEG.

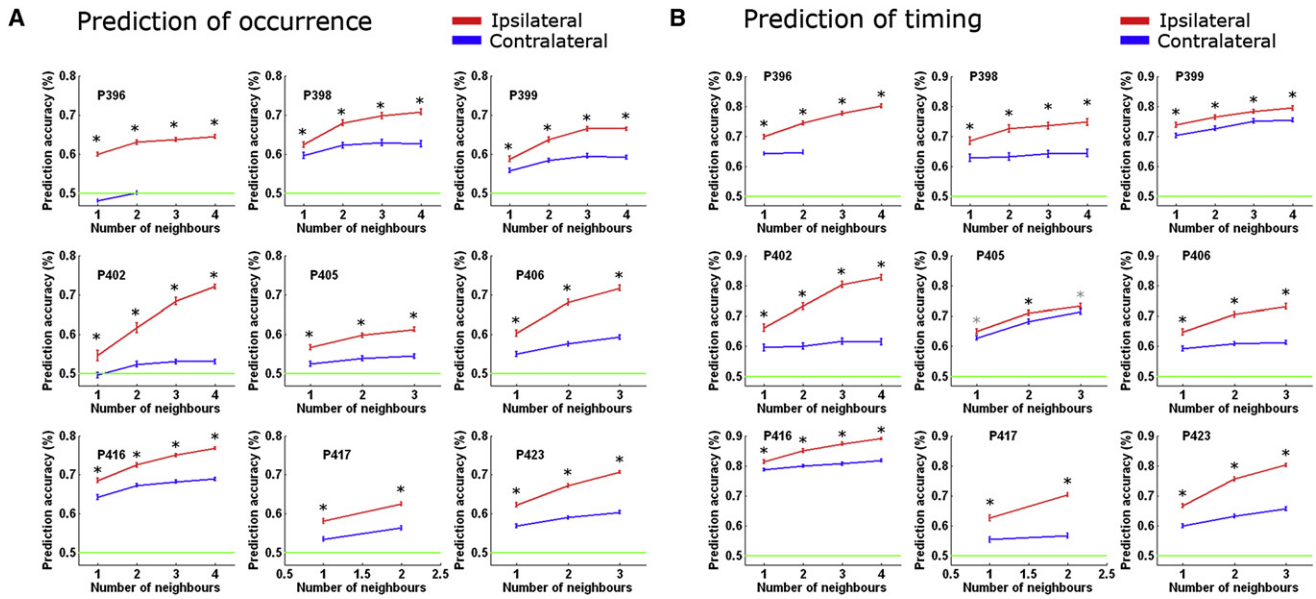

Figure 8. Afferent Information Predicts Occurrence and Timing of Activity Onsets in Individual Slow Waves

(A) Predicting occurrence of individual amygdala slow waves with information about slow waves in other limbic regions. Each subpanel shows prediction accuracies for one patient using either ipsilateral (red) or contralateral (blue) information, as a function of the number of regions made available to the classifier. Green horizontal line shows chance prediction at 50%. Error bars denote SEM across 100 classifier iterations in which training and testing datasets (individual waves) as well as the identity of available neighbors were shuffled. Black and gray asterisks denote significant differences in prediction accuracy ($p < 0.001$ and $p < 0.05$ respectively, paired t test). Note that in all nine patients, prediction was significantly more accurate using ipsilateral information, reflecting the fact that bulk anatomical projections to amygdala arrive from ipsilateral brain regions ($p < 1 \times 10^{-39}$ in all nine individuals, paired t test, n = 100 classifier iterations).

(B) Same as above when predicting the timing of individual amygdala slow waves (before or after slow waves in parietal scalp electrode Pz). Timing prediction was likewise more accurate based on ipsilateral information ($p < 1.4 \times 10^{-7}$ in eight individuals and $p = 0.02$ in ninth individual, paired t test, n = 100 classifier iterations).

We also examined whether hippocampal SWR bursts may be driving responses in mPFC on a fine time scale, as suggested recently (Wierzynski et al., 2009). Our results reveal a clear tendency of hippocampal ripples to occur around ON periods of slow waves (Figure S7D), as reported previously (Clemens et al., 2007; Molle et al., 2006; Sirota et al., 2003). Moreover, delayed and attenuated spike discharges were observed in entorhinal cortex compared with hippocampus (Figures S7E and S7G). Since the entorhinal cortex provides both the major input to and receives output from the hippocampus, our results support the notion that ripples reflect hippocampal output (Chrobak and Buzsaki, 1996). Local effects of hippocampal output within the MTL are in line with a recent human study reporting some incidences of delayed gamma bursts in parahippocampal cortex following hippocampal ripples (Le Van Quyen et al., 2010). However, transient firing in mPFC units was not found following ripple occurrence (Figures S7E and S7G). The apparent discrepancy with (Wierzynski et al., 2009) is most likely related to the fact that our data represent a different neuronal population in the mPFC where neuronal activity is highly modulated by slow waves (compare to their Figure 1), but differences in species and electrode locations may contribute as well.

More generally, the direction of the cortico-hippocampal dialogue in sleep has been a hotly debated issue. An influential suggestion has been that signals propagate from cortex to hippocampus during wakefulness and from hippocampus to cortex during sleep (Buzsaki, 1998). Since declarative memories become progressively more resistant to hippocampal damage, it is thought that the hippocampus "transfers" such memories to the cortex by replaying activity patterns during SWRs in sleep (Lee and Wilson, 2002). The current results add to existing evidence showing that during NREM sleep neural activity propagates predominantly from the neocortex to the hippocampus (Hahn et al., 2007; Isomura et al., 2006; Ji and Wilson, 2007; Molle et al., 2006; Sirota et al., 2003). Future studies are needed to determine whether within this robust cortico-hippocampal broadcast there may be islands of functionally relevant hippocampo-cortical transmission (Tononi et al., 2006).

Cumulative Synaptic Input Determines Transitions to ON Periods

While slow waves reflect spontaneous alternations of activity and silence in corticothalamic networks, what causes the transition from silence to activity in a given brain region remains unclear. Several scenarios could explain the source of transitions at the network level. One possibility is that whether and when a given region will transition into an ON period is determined by a global process such as subcortical common input, which could serve as a main "switch." However, since most slow waves occur locally and since slow oscillations are also observed in vitro (Sanchez-Vives and McCormick, 2000), such a global mechanism seems implausible. A second possibility is

that transitions to activity are stochastic and driven by intrinsic processes within each region. For example, currents that are activated close to the resting membrane potential (such as the hyperpolarization-activated depolarizing current; McCormick and Pape, 1990) could lead neurons to discharge during OFF periods and initiate activity that would then spread within a region, irrespective of other brain regions. A third possibility is that synaptic drive gradually builds up prior to the onset of ON periods, so that whether and when a region becomes active reflects the cumulative input to that region (Chauvette et al., 2010).

By capitalizing on the amygdala, for which ipsilateral projections constitute the dominant input (Amaral et al., 1992; McDonald, 1998), we show that predicting individual ON periods is significantly more accurate when based on information from ipsilateral limbic regions compared with contralateral limbic regions. This suggests that the state of afferent regions provides particularly relevant information about the transition into an active state. Moreover, within ipsilateral regions, the prediction grew stronger depending on the number of inputs made available to the classifier, whereas this effect was much weaker for contralateral regions. Taken together, our results suggest that the cumulative synaptic input to a given region is a major determinant of whether and when it will enter an active state.

Potential Confounding Factors

Our data were recorded in medicated epilepsy patients in whom abnormal events during seizure-free periods may affect brain activity in slow wave sleep (Dinner and Lüders, 2001). Inter-ictal epileptiform activity, as well as antiepileptic drugs (AEDs) and their adjustments could affect sleep in general, and the nature of slow waves in particular. Therefore, it was imperative to confirm that our results could indeed be generalized to the healthy population, and multiple observations strongly suggest that this is indeed the case. First, our overnight recordings were performed before routine tapering of AEDs to ensure a less significant contribution of epileptiform activities. Second, sleep measures were within the expected normal range, including distribution of sleep stages, NREM-REM cycles, and EEG power spectra of each sleep stage (Figure S1). By specifically detecting pathological interictal spikes and paroxysmal discharges and separating them from physiological sleep slow waves, several additional features were revealed that clearly distinguish these phenomena (Figure S2). Third, the occurrence rate of paroxysmal discharges was highly variable across channels, limited in its spatial extent, and entirely absent in some channels. By contrast, the number of physiological sleep slow waves was highly consistent across channels and in line with that reported in healthy individuals. Fourth, all the results reported here, including a tight relationship between EEG slow waves and unit activities, local slow waves and spindles, and slow wave propagation, could be observed in every individual despite drastically different clinical profiles (Table S1B). This consistency argues against contributions of idiosyncratic epileptiform events, for which underlying unit activities are highly variable (Wyler et al., 1982). Fifth, comparing the morphology of sleep slow waves and interictal paroxysmal discharges revealed a significant difference in the waveform shape of pathological events. Sixth and most importantly, our analysis of spiking activities underlying physiological versus pathological waves revealed significant differences, confirming our ability to separate sleep slow waves from epileptic events (Figure S2). Specifically, elevated firing rates around interictal spikes, presumably reflecting a high degree of synchrony among neurons within the epileptogenic focus (Wyler et al., 1982) led to highly asymmetric patterns.

Functional Significance

The observation that most slow waves are local has several implications. Although sleep slow waves are the most conspicuous electrical activity pattern observed during sleep, it is not yet clear whether they serve a specific function. However, since EEG SWA is tightly regulated (i.e., increases with time awake and decreases during sleep) and is a reliable indicator of sleep need (Borbely and Achermann, 1999), it may serve some restorative function. Moreover, slow wave deprivation (Aeschbach et al., 2008; Landsness et al., 2009) and enhancement (Marshall et al., 2006) impair and improve learning, respectively, suggesting that slow waves, or perhaps spindle, gamma, and ripple oscillations that are grouped by the slow oscillation, may play a role in memory consolidation (Diekelmann and Born, 2010; Stickgold and Walker, 2007; Tononi and Cirelli, 2006). The present results offer some constraints on how slow waves may aid memory consolidation. The fact that the up-state in one brain region is usually out of phase with respect to other brain regions constrains the nature of such information transfer during up-states. In addition, when slow waves do occur across several brain regions, they have a clear tendency to propagate across typical paths so that they occur with typical time delays across different regions. This trait imposes a directionality to plasticity-related processes, and such propagating waves may play a role in time-dependent synaptic plasticity (Ermentrout and Kleinfeld, 2001), such as spike timing-dependent plasticity (Caporale and Dan, 2008).

The results also refine our view of what happens in the brain in late sleep at the end of the night. Once sleep pressure has largely dissipated, NREM sleep is dominated at the EEG level by low-amplitude slow waves (Riedner et al., 2007). As shown here, low-amplitude scalp slow waves do not reflect small waves occurring simultaneously across the brain, but mostly represent local waves occurring out of phase across different brain regions. Therefore, whatever functional process is supported by slow waves, it occurs more and more locally toward the end of sleep. Moreover, the fact that in late sleep many brain regions remain in an ON state while only a minority of areas are in an OFF state may not be unrelated to the increased occurrence and intensity of dreaming in NREM sleep toward the end of the night (Nir and Tononi, 2010). Finally, local slow waves observed in wake are usually interpreted as reflecting pathology (e.g., lesions). Given that local slow waves are the norm in sleep, similar events in wake could be re-interpreted as reflecting ''piecemeal-sleep.''

The finding that most sleep spindles are local may also bear functional implications. That spindle oscillations in cortico-thalamic-cortical loops maintain regional specificity during sleep provides further evidence that spontaneous activity during

resting states is locally organized. Thus, rather than just implementing a global "thalamic gate," sleep spindle oscillations may contribute to synaptic plasticity in a circuit-specific manner.

In summary, the current results further extend and refine our evolving view of neuronal activity in sleep by showing that the two fundamental brain oscillations of sleep—slow waves and spindles—occur mostly locally. It may be that a functional disconnection among different sectors of the corticothalamic system may represent a unique feature of sleep, with as yet unexplored functional consequences.

EXPERIMENTAL PROCEDURES

Subjects and Sleep Studies

Thirteen patients with intractable epilepsy were implanted with intracranial depth electrodes to identify seizure foci for potential surgical treatment. Electrode location was based solely on clinical criteria. All patients provided written informed consent to participate in the research study, under the approval of the Medical Institutional Review Board at UCLA. Sleep studies were conducted on the hospital ward 48–72 hr after surgery and lasted 7 hr on average, and sleep-wake stages were scored according to established guidelines. The montage included two EOG electrodes; two EMG electrodes; scalp electrodes at C3, C4, Pz, and Fz; two earlobe electrodes used for reference; and continuous video monitoring.

Data Acquisition and Spike Sorting

In each patient, 8–12 depth electrodes were implanted targeting medial brain areas. Both scalp and depth EEG data were continuously recorded at a sampling rate of 2 kHz, bandpass-filtered between 0.1 and 500 Hz, and re-referenced offline to the mean signal recorded from the earlobes. Intracranial/depth EEG refers to data recorded from the most medial platinum contact along the shaft (Figure 1D, blue). Each electrode terminated in eight 40-μm platinum-iridium microwires from which extracellular signals were continuously recorded (referenced locally to a ninth noninsulated microwire) at a sampling rate of 28/30 kHz and bandpass-filtered between 1 and 6000 Hz. Action potentials were detected by high-pass filtering the extracellular recordings above 300 Hz and applying a threshold at 5 SD above the median noise level. Detected events were further categorized as noise, single-unit, or multiunit events using superparamagnetic clustering, as in (Nir et al., 2008). Unit stability throughout sleep recordings was confirmed by verifying that spike waveforms and inter-spike-interval distributions were consistent and distinct throughout the night (Figure S3B). For visualizations purposes in Figures 1F, 4A, and 7D and Figure S4, multiunit activity (MUA) traces were extracted from microwire recordings by filtering the signals offline between 300 and 3000 Hz.

Analysis of Slow Waves, Sleep Spindles, and Hippocampal Ripples in Depth EEG Data

Detection details for all events are given in the Supplemental Experimental Procedures. Putative slow waves were subdivided into those preceded (within 1 s) by an interictal spike ("paroxysmal" discharges) and those unrelated to paroxysmal events ("physiological" sleep slow waves). Physiological slow waves occurring near-simultaneously across channels (within ± 400 ms, Figure S4) were considered "concordant" events (Figure 4). For slow wave propagation (Figure 7), we focused on events identified in Fz and in intracranial recordings of at least three brain structures, although the results were highly robust to the exact detection parameters and to other examinations (Figure S6). To compare timing of unit discharges within MTL (Figure 5F), we defined time zero based on the positive peak of EEG slow waves in parahippocampal gyrus (9/13 subjects) or entorhinal cortex (4/13 subjects). For analysis of local spindles, spectrograms were computed in ± 1 s intervals around peak spindle power, using a short-time Fourier transform with a window of 744 ms and 95% overlap, and normalizing power relative to random intervals as in (Sirota et al., 2003).

Relationship between Neuronal Spiking and Sleep Slow Waves

Phased-locked spiking (Figure 3D) was assessed by extracting the instantaneous phase of the depth EEG filtered between 0.5–4 Hz ± 500 ms surrounding slow wave positive peaks via the Hilbert transform, testing for nonuniformity of the phase distribution of spike occurrences using Rayleigh's test, and determining critical p values using shuffled data to control for asymmetries in the EEG waveforms (Figure S3). Slow-wave-triggered averaging was conducted for each unit separately using the highest amplitude slow waves in each channel (top 20%). The timing and magnitude of firing rate modulations were defined based on the maxima/minima using 20 ms bins. Propagation in unit activities were evaluated across all significantly phase-locked units within a region (Figures 7E and 7F, left; Figure S7F), or for individual units separately using 20 ms bins (Figures 7E and 7F, right). Statistical significance of time differences between spiking activities of individual units in distinct brain structures (Figures 4E and 4F) was evaluated via bootstrapping by (1) assigning a random anatomical label to each neuron separately (either frontal or MTL for Figure S6G, either PH or HC for "within MTL" analysis in Figure S6H), (2) creating surrogate groups with the same number of units as the real data, and (3) computing the random time offset between the two groups as was done for the real data (Figure S6).

Dynamics throughout Sleep

In five individuals exhibiting a clear homeostatic decline of SWA during sleep, we analyzed slow waves, K-complexes, and sleep spindle separately in early and late NREM sleep (Figure S1D). Putative K-complexes were detected in Fz recordings as isolated slow waves (within ± 3 s) with peak-to-peak amplitude >75 μV.

Prediction of Individual Slow Waves via Linear Classifier

Classification was performed with a support vector machine using a linear (dot product) kernel, using data from 17 hemispheres of nine individuals in which signals from amygdala and other limbic structures were recorded. The occurrence, amplitude, and timing of transitions into population ON periods (positive peaks in depth EEG) were used to train (80% of events) and test (20% of events) a linear classifier using either ipsilateral or contralateral limbic information. Differences between ipsilateral versus contralateral prediction accuracy were evaluated using a paired t test with df = 100 (number of classifier iterations) for each number of neighbors separately.

SUPPLEMENTAL INFORMATION

Supplemental information includes seven figures, one table, and Supplemental Experimental Procedures and can be found with this article online at doi:10.1016/j.neuron.2011.02.043.

ACKNOWLEDGMENTS

We thank the patients for their cooperation; E. Behnke, T. Fields, V. Isiaka, D. Pourshaban, R. Mukamel, A. Tankus, N. Suthana, and K. Shattuck for assistance with data acquisition; B. Salaz and I. Wainwright for administrative help; B. Riedner for slow wave detection algorithms and valuable input; and M. Murphy and F. Ferrarelli for discussions and comments. This work was supported by the European Molecular Biology Organization and Human Frontier Science Program Organization long-term fellowships (support to Y.N.), the Brainpower for Israel Fund (support to Y.N.), National Institute of Health Director's Pioneer Award (support to G.T.), NIH (grants P20 MH077967 and R01 NS055185 to G.T.), and National Institute of Neurological Disorders and Stroke (grants to R.S. and I.F.).

Accepted: January 26, 2011
Published: April 13, 2011

REFERENCES

Achermann, P., and Borbely, A.A. (1998). Temporal evolution of coherence and power in the human sleep electroencephalogram. J. Sleep Res. *7* (*Suppl 1*), 36–41.

Aeschbach, D., Cutler, A.J., and Ronda, J.M. (2008). A role for non-rapid-eye-movement sleep homeostasis in perceptual learning. J. Neurosci. *28*, 2766–2772.

Amaral, D.G., Price, J.L., Pitkanen, A., and Carmichael, S.T. (1992). Anatomical organization of the primate amygdala. In The Amygdala: Neurobiological Aspects of Emotion, Memory, and Mental Dysfunction, J.P. Aggleton, ed. (New York: Wiley-Liss), pp. 1–66.

Amzica, F., and Steriade, M. (1995a). Disconnection of intracortical synaptic linkages disrupts synchronization of a slow oscillation. J. Neurosci. *15*, 4658–4677.

Amzica, F., and Steriade, M. (1995b). Short- and long-range neuronal synchronization of the slow (< 1 Hz) cortical oscillation. J. Neurophysiol. *73*, 20–38.

Amzica, F., and Steriade, M. (1998). Cellular substrates and laminar profile of sleep K-complex. Neuroscience *82*, 671–686.

Anderer, P., Klosch, G., Gruber, G., Trenker, E., Pascual-Marqui, R.D., Zeitlhofer, J., Barbanoj, M.J., Rappelsberger, P., and Saletu, B. (2001). Low-resolution brain electromagnetic tomography revealed simultaneously active frontal and parietal sleep spindle sources in the human cortex. Neuroscience *103*, 581–592.

Bassetti, C., Vella, S., Donati, F., Wielepp, P., and Weder, B. (2000). SPECT during sleepwalking. Lancet *356*, 484–485.

Borbely, A.A., and Achermann, P. (1999). Sleep homeostasis and models of sleep regulation. J. Biol. Rhythms *14*, 557–568.

Braun, A.R., Balkin, T.J., Wesenten, N.J., Carson, R.E., Varga, M., Baldwin, P., Selbie, S., Belenky, G., and Herscovitch, P. (1997). Regional cerebral blood flow throughout the sleep-wake cycle: An H2(15)O PET study. Brain *120* (Pt 7), 1173–1197.

Buzsaki, G. (1998). Memory consolidation during sleep: A neurophysiological perspective. J. Sleep Res. *7* (*Suppl 1*), 17–23.

Caderas, M., Niedermeyer, E., Uematsu, S., Long, D.M., and Nastalski, J. (1982). Sleep spindles recorded from deep cerebral structures in man. Clin. Electroencephalogr. *13*, 216–225.

Campbell, I.G. (2009). EEG recording and analysis for sleep research. Curr. Protoc. Neurosci. *Chapter 10*, Unit 10.2.

Caporale, N., and Dan, Y. (2008). Spike timing-dependent plasticity: A Hebbian learning rule. Annu. Rev. Neurosci. *31*, 25–46.

Cash, S.S., Halgren, E., Dehghani, N., Rossetti, A.O., Thesen, T., Wang, C., Devinsky, O., Kuzniecky, R., Doyle, W., Madsen, J.R., et al. (2009). The human K-complex represents an isolated cortical down-state. Science *324*, 1084–1087.

Cavada, C., Company, T., Tejedor, J., Cruz-Rizzolo, R.J., and Reinoso-Suarez, F. (2000). The anatomical connections of the macaque monkey orbitofrontal cortex. A review. Cereb. Cortex *10*, 220–242.

Chauvette, S., Volgushev, M., and Timofeev, I. (2010). Origin of active states in local neocortical networks during slow sleep oscillation. Cereb, Cortex. *20*, 2660–2674.

Chrobak, J.J., and Buzsaki, G. (1996). High-frequency oscillations in the output networks of the hippocampal-entorhinal axis of the freely behaving rat. J. Neurosci. *16*, 3056–3066.

Clemens, Z., Molle, M., Eross, L., Barsi, P., Halasz, P., and Born, J. (2007). Temporal coupling of parahippocampal ripples, sleep spindles and slow oscillations in humans. Brain *130*, 2868–2878.

Colrain, I.M. (2005). The K-complex: A 7-decade history. Sleep *28*, 255–273.

Contreras, D., Destexhe, A., Sejnowski, T.J., and Steriade, M. (1996). Control of spatiotemporal coherence of a thalamic oscillation by corticothalamic feedback. Science *274*, 771–774.

Contreras, D., Destexhe, A., and Steriade, M. (1997). Spindle oscillations during cortical spreading depression in naturally sleeping cats. Neuroscience *77*, 933–936.

Contreras, D., and Steriade, M. (1995). Cellular basis of EEG slow rhythms: A study of dynamic corticothalamic relationships. J. Neurosci. *15*, 604–622.

Crunelli, V., and Hughes, S.W. (2010). The slow (<1 Hz) rhythm of non-REM sleep: A dialogue between three cardinal oscillators. Nat. Neurosci. *13*, 9–17.

Csercsa, R., Dombovari, B., Fabo, D., Wittner, L., Eross, L., Entz, L., Solyom, A., Rasonyi, G., Szucs, A., Kelemen, A., et al. (2010). Laminar analysis of slow wave activity in humans. Brain *133*, 2814–2829.

Dang-Vu, T.T., Desseilles, M., Laureys, S., Degueldre, C., Perrin, F., Phillips, C., Maquet, P., and Peigneux, P. (2005). Cerebral correlates of delta waves during non-REM sleep revisited. Neuroimage *28*, 14–21.

Dang-Vu, T.T., Schabus, M., Desseilles, M., Albouy, G., Boly, M., Darsaud, A., Gais, S., Rauchs, G., Sterpenich, V., Vandewalle, G., et al. (2008). Spontaneous neural activity during human slow wave sleep. Proc. Natl. Acad. Sci. USA *105*, 15160–15165.

Dehghani, N., Cash, S.S., Chen, C.C., Hagler, D.J., Jr., Huang, M., Dale, A.M., and Halgren, E. (2010). Divergent cortical generators of MEG and EEG during human sleep spindles suggested by distributed source modeling. PLoS ONE *5*, e11454.

Destexhe, A., and Contreras, D. (2006). Neuronal computations with stochastic network states. Science *314*, 85–90.

Destexhe, A., Contreras, D., and Steriade, M. (1999). Spatiotemporal analysis of local field potentials and unit discharges in cat cerebral cortex during natural wake and sleep states. J. Neurosci. *19*, 4595–4608.

Destexhe, A., Hughes, S.W., Rudolph, M., and Crunelli, V. (2007). Are corticothalamic "up" states fragments of wakefulness? Trends Neurosci. *30*, 334–342.

Diekelmann, S., and Born, J. (2010). The memory function of sleep. Nat. Rev. Neurosci. *11*, 114–126.

Dinner, D.S., and Lüders, H.O., eds. (2001). Epilepsy and Sleep: Physiological and Clinical Relationships (San Diego, CA: Academic Press).

Ermentrout, G.B., and Kleinfeld, D. (2001). Traveling electrical waves in cortex: insights from phase dynamics and speculation on a computational role. Neuron *29*, 33–44.

Esser, S.K., Huber, R., Massimini, M., Peterson, M.J., Ferrarelli, F., and Tononi, G. (2006). A direct demonstration of cortical LTP in humans: a combined TMS/EEG study. Brain Res. Bull. *69*, 86–94.

Finelli, L.A., Borbely, A.A., and Achermann, P. (2001). Functional topography of the human nonREM sleep electroencephalogram. Eur. J. Neurosci. *13*, 2282–2290.

Gottselig, J.M., Bassetti, C.L., and Achermann, P. (2002). Power and coherence of sleep spindle frequency activity following hemispheric stroke. Brain *125*, 373–383.

Hagmann, P., Cammoun, L., Gigandet, X., Meuli, R., Honey, C.J., Wedeen, V.J., and Sporns, O. (2008). Mapping the structural core of human cerebral cortex. PLoS Biol. *6*, e159.

Hahn, T.T., Sakmann, B., and Mehta, M.R. (2007). Differential responses of hippocampal subfields to cortical up-down states. Proc. Natl. Acad. Sci. USA *104*, 5169–5174.

Huber, R., Ghilardi, M.F., Massimini, M., Ferrarelli, F., Riedner, B.A., Peterson, M.J., and Tononi, G. (2006). Arm immobilization causes cortical plastic changes and locally decreases sleep slow wave activity. Nat. Neurosci. *9*, 1169–1176.

Huber, R., Ghilardi, M.F., Massimini, M., and Tononi, G. (2004). Local sleep and learning. Nature *430*, 78–81.

Iber, C., Ancoli-Israel, S., Chesson, A.L., and Quan, S.F. (2007). The AASM Manual for the Scoring of Sleep and Associated Events: Rules, Terminology and Technical Specifications (Westchester, IL: American Association of Sleep Medicine).

Isomura, Y., Sirota, A., Ozen, S., Montgomery, S., Mizuseki, K., Henze, D.A., and Buzsaki, G. (2006). Integration and segregation of activity in entorhinal-hippocampal subregions by neocortical slow oscillations. Neuron *52*, 871–882.

Ji, D., and Wilson, M.A. (2007). Coordinated memory replay in the visual cortex and hippocampus during sleep. Nat. Neurosci. *10*, 100–107.

Jones, B.E. (2005). From waking to sleeping: Neuronal and chemical substrates. Trends Pharmacol. Sci. *26*, 578–586.

Jones, E.G. (2009). Synchrony in the interconnected circuitry of the thalamus and cerebral cortex. Ann. N Y Acad. Sci. *1157*, 10–23.

Khazipov, R., Sirota, A., Leinekugel, X., Holmes, G.L., Ben-Ari, Y., and Buzsaki, G. (2004). Early motor activity drives spindle bursts in the developing somatosensory cortex. Nature *432*, 758–761.

Kristiansen, K., and Courtois, G. (1949). Rhythmic electrical activity from isolated cerebral cortex. Electroencephalogr. Clin. Neurophysiol. *1*, 265–272.

Krueger, J.M., Rector, D.M., Roy, S., Van Dongen, H.P., Belenky, G., and Panksepp, J. (2008). Sleep as a fundamental property of neuronal assemblies. Nat. Rev. Neurosci. *9*, 910–919.

Landsness, E.C., Crupi, D., Hulse, B.K., Peterson, M.J., Huber, R., Ansari, H., Coen, M., Cirelli, C., Benca, R.M., Ghilardi, M.F., and Tononi, G. (2009). Sleep-dependent improvement in visuomotor learning: A causal role for slow waves. Sleep *32*, 1273–1284.

Le Van Quyen, M., Staba, R., Bragin, A., Dickson, C., Valderrama, M., Fried, I., and Engel, J. (2010). Large-scale microelectrode recordings of high-frequency gamma oscillations in human cortex during sleep. J. Neurosci. *30*, 7770–7782.

Lee, A.K., and Wilson, M.A. (2002). Memory of sequential experience in the hippocampus during slow wave sleep. Neuron *36*, 1183–1194.

Loomis, A.L., Harvey, E.N., and Hobart, G. (1935). Potential rhythms of the cerebral cortex during sleep. Science *81*, 597–598.

Magnin, M., Rey, M., Bastuji, H., Guillemant, P., Mauguiere, F., and Garcia-Larrea, L. (2010). Thalamic deactivation at sleep onset precedes that of the cerebral cortex in humans. Proc. Natl. Acad. Sci. USA *107*, 3829–3833.

Mahowald, M.W., and Schenck, C.H. (2005). Insights from studying human sleep disorders. Nature *437*, 1279–1285.

Maquet, P. (2000). Functional neuroimaging of normal human sleep by positron emission tomography. J. Sleep Res. *9*, 207–231.

Marshall, L., Helgadottir, H., Molle, M., and Born, J. (2006). Boosting slow oscillations during sleep potentiates memory. Nature *444*, 610–613.

Massimini, M., Huber, R., Ferrarelli, F., Hill, S., and Tononi, G. (2004). The sleep slow oscillation as a traveling wave. J. Neurosci. *24*, 6862–6870.

McCormick, D.A., and Bal, T. (1997). Sleep and arousal: Thalamocortical mechanisms. Annu. Rev. Neurosci. *20*, 185–215.

McCormick, D.A., and Pape, H.C. (1990). Properties of a hyperpolarization-activated cation current and its role in rhythmic oscillation in thalamic relay neurones. J. Physiol. *431*, 291–318.

McDonald, A.J. (1998). Cortical pathways to the mammalian amygdala. Prog. Neurobiol. *55*, 257–332.

Mohajerani, M.H., McVea, D.A., Fingas, M., and Murphy, T.H. (2010). Mirrored bilateral slow-wave cortical activity within local circuits revealed by fast bihemispheric voltage-sensitive dye imaging in anesthetized and awake mice. J. Neurosci. *30*, 3745–3751.

Molle, M., Marshall, L., Gais, S., and Born, J. (2002). Grouping of spindle activity during slow oscillations in human non-rapid eye movement sleep. J. Neurosci. *22*, 10941–10947.

Molle, M., Yeshenko, O., Marshall, L., Sara, S.J., and Born, J. (2006). Hippocampal sharp wave-ripples linked to slow oscillations in rat slow-wave sleep. J. Neurophysiol. *96*, 62–70.

Mukhametov, L.M., Supin, A.Y., and Polyakova, I.G. (1977). Interhemispheric asymmetry of the electroencephalographic sleep patterns in dolphins. Brain Res. *134*, 581–584.

Murphy, M., Riedner, B.A., Huber, R., Massimini, M., Ferrarelli, F., and Tononi, G. (2009). Source modeling sleep slow waves. Proc. Natl. Acad. Sci. USA *106*, 1608–1613.

Nir, Y., Mukamel, R., Dinstein, I., Privman, E., Harel, M., Fisch, L., Gelbard-Sagiv, H., Kipervasser, S., Andelman, F., Neufeld, M.Y., et al. (2008). Interhemispheric correlations of slow spontaneous neuronal fluctuations revealed in human sensory cortex. Nat. Neurosci. *11*, 1100–1108.

Nir, Y., and Tononi, G. (2010). Dreaming and the brain: From phenomenology to neurophysiology. Trends Cogn. Sci. *14*, 88–100.

Nishida, M., and Walker, M.P. (2007). Daytime naps, motor memory consolidation and regionally specific sleep spindles. PLoS ONE *2*, e341.

Noda, H., and Adey, W.R. (1970). Firing of neuron pairs in cat association cortex during sleep and wakefulness. J. Neurophysiol. *33*, 672–684.

Pare, D., Collins, D.R., and Pelletier, J.G. (2002). Amygdala oscillations and the consolidation of emotional memories. Trends. Cogn. Sci. *6*, 306–314.

Rattenborg, N.C., Amlaner, C.J., and Lima, S.L. (2001). Unilateral eye closure and interhemispheric EEG asymmetry during sleep in the pigeon (*Columba livia*). Brain Behav. Evol. *58*, 323–332.

Riedner, B.A., Vyazovskiy, V.V., Huber, R., Massimini, M., Esser, S., Murphy, M., and Tononi, G. (2007). Sleep homeostasis and cortical synchronization: III. A high-density EEG study of sleep slow waves in humans. Sleep *30*, 1643–1657.

Rubio-Garrido, P., Perez-de-Manzo, F., Porrero, C., Galazo, M.J., and Clasca, F. (2009). Thalamic input to distal apical dendrites in neocortical layer 1 is massive and highly convergent. Cereb. Cortex. *19*, 2380–2395.

Sanchez-Vives, M.V., and McCormick, D.A. (2000). Cellular and network mechanisms of rhythmic recurrent activity in neocortex. Nat. Neurosci. *3*, 1027–1034.

Sejnowski, T.J., and Destexhe, A. (2000). Why do we sleep? Brain Res. *886*, 208–223.

Shu, Y., Hasenstaub, A., and McCormick, D.A. (2003). Turning on and off recurrent balanced cortical activity. Nature *423*, 288–293.

Siegel, J.M. (2009). Sleep viewed as a state of adaptive inactivity. Nat. Rev. Neurosci. *10*, 747–753.

Sirota, A., and Buzsaki, G. (2005). Interaction between neocortical and hippocampal networks via slow oscillations. Thalamus Relat. Syst. *3*, 245–259.

Sirota, A., Csicsvari, J., Buhl, D., and Buzsaki, G. (2003). Communication between neocortex and hippocampus during sleep in rodents. Proc. Natl. Acad. Sci. USA *100*, 2065–2069.

Steriade, M. (2000). Corticothalamic resonance, states of vigilance and mentation. Neuroscience *101*, 243–276.

Steriade, M. (2003). Neuronal substrates of sleep and epilepsy (Cambridge, UK: Cambridge University Press).

Steriade, M., Contreras, D., Curro Dossi, R., and Nunez, A. (1993a). The slow (< 1 Hz) oscillation in reticular thalamic and thalamocortical neurons: Scenario of sleep rhythm generation in interacting thalamic and neocortical networks. J. Neurosci. *13*, 3284–3299.

Steriade, M., Nunez, A., and Amzica, F. (1993b). Intracellular analysis of relations between the slow (< 1 Hz) neocortical oscillation and other sleep rhythms of the electroencephalogram. J. Neurosci. *13*, 3266–3283.

Steriade, M., Nunez, A., and Amzica, F. (1993c). A novel slow (< 1 Hz) oscillation of neocortical neurons in vivo: Depolarizing and hyperpolarizing components. J. Neurosci. *13*, 3252–3265.

Steriade, M., Timofeev, I., and Grenier, F. (2001). Natural waking and sleep states: A view from inside neocortical neurons. J. Neurophysiol. *85*, 1969–1985.

Stickgold, R., and Walker, M.P. (2007). Sleep-dependent memory consolidation and reconsolidation. Sleep Med. *8*, 331–343.

Terzaghi, M., Sartori, I., Tassi, L., Didato, G., Rustioni, V., LoRusso, G., Manni, R., and Nobili, L. (2009). Evidence of dissociated arousal states during NREM parasomnia from an intracerebral neurophysiological study. Sleep *32*, 409–412.

Timofeev, I., Grenier, F., Bazhenov, M., Sejnowski, T.J., and Steriade, M. (2000). Origin of slow cortical oscillations in deafferented cortical slabs. Cereb. Cortex *10*, 1185–1199.

Timofeev, I., Grenier, F., and Steriade, M. (2001). Disfacilitation and active inhibition in the neocortex during the natural sleep-wake cycle: An intracellular study. Proc. Natl. Acad. Sci. USA *98*, 1924–1929.

Timofeev, I., and Steriade, M. (1996). Low-frequency rhythms in the thalamus of intact-cortex and decorticated cats. J. Neurophysiol. *76*, 4152–4168.

Tononi, G., and Cirelli, C. (2006). Sleep function and synaptic homeostasis. Sleep Med. Rev. *10*, 49–62.

Tononi, G., Massimini, M., and Riedner, B.A. (2006). Sleepy dialogues between cortex and hippocampus: Who talks to whom? Neuron *52*, 748–749.

Volgushev, M., Chauvette, S., Mukovski, M., and Timofeev, I. (2006). Precise long-range synchronization of activity and silence in neocortical neurons during slow-wave oscillations. J. Neurosci. *26*, 5665–5672.

Vyazovskiy, V., Borbely, A.A., and Tobler, I. (2000). Unilateral vibrissae stimulation during waking induces interhemispheric EEG asymmetry during subsequent sleep in the rat. J. Sleep. Res. *9*, 367–371.

Vyazovskiy, V.V., Faraguna, U., Cirelli, C., and Tononi, G. (2009a). Triggering slow waves during NREM sleep in the rat by intracortical electrical stimulation: Effects of sleep/wake history and background activity. J. Neurophysiol. *101*, 1921–1931.

Vyazovskiy, V.V., Olcese, U., Lazimy, Y.M., Faraguna, U., Esser, S.K., Williams, J.C., Cirelli, C., and Tononi, G. (2009b). Cortical firing and sleep homeostasis. Neuron *63*, 865–878.

Vyazovskiy, V.V., Olcese, U., Hanlon, E.C., Nir, Y., Cirelli, C., and Tononi, G. (2011). Local sleep in awake rats. Nature, in press. 10.1038/nature10009.

Wagner, T., Axmacher, N., Lehnertz, K., Elger, C.E., and Fell, J. (2010). Sleep-dependent directional coupling between human neocortex and hippocampus. Cortex *46*, 256–263.

Werth, E., Achermann, P., and Borbely, A.A. (1997). Fronto-occipital EEG power gradients in human sleep. J. Sleep Res. *6*, 102–112.

Wierzynski, C.M., Lubenov, E.V., Gu, M., and Siapas, A.G. (2009). State-dependent spike-timing relationships between hippocampal and prefrontal circuits during sleep. Neuron *61*, 587–596.

Wolansky, T., Clement, E.A., Peters, S.R., Palczak, M.A., and Dickson, C.T. (2006). Hippocampal slow oscillation: A novel EEG state and its coordination with ongoing neocortical activity. J. Neurosci. *26*, 6213–6229.

Wyler, A.R., Ojemann, G.A., and Ward, A.A., Jr. (1982). Neurons in human epileptic cortex: Correlation between unit and EEG activity. Ann. Neurol. *11*, 301–308.

Zikopoulos, B., and Barbas, H. (2007). Parallel driving and modulatory pathways link the prefrontal cortex and thalamus. PLoS One *2*, e848.